INTERNATIONAL JOURNAL FOR NUMERICAL METHODS IN ENGINEERING
Int. J. Numer. Meth. Engng 2006; **68**:993–1011
Published online 27 April 2006 in Wiley InterScience (www.interscience.wiley.com). DOI: 10.1002/nme.1743

Scale-related topology optimization of cellular materials and structures

Weihong Zhang*,† and Shiping Sun

Sino-French Laboratory of Concurrent Engineering, Northwestern Polytechnical University, 710072 Xi'an, China

SUMMARY

The integrated optimization of lightweight cellular materials and structures are discussed in this paper. By analysing the basic features of such a two-scale problem, it is shown that the optimal solution strongly depends upon the scale effect modelling of the periodic microstructure of material unit cell (MUC), i.e. the so-called representative volume element (RVE). However, with the asymptotic homogenization method used widely in actual topology optimization procedure, effective material properties predicted can give rise to limit values depending upon only volume fractions of solid phases, properties and spatial distribution of constituents in the microstructure regardless of scale effect. From this consideration, we propose the design element (DE) concept being able to deal with conventional designs of materials and structures in a unified way. By changing the scale and aspect ratio of the DE, scale-related effects of materials and structures are well revealed and distinguished in the final results of optimal design patterns. To illustrate the proposed approach, numerical design problems of 2D layered structures with cellular core are investigated. Copyright © 2006 John Wiley & Sons, Ltd.

KEY WORDS: scale effect; topology optimization; cellular material design; unit cell; homogenization method

1. INTRODUCTION

Cellular solids are ultra-lightweight materials that find wide applications in aerospace and automotive industries due to their particular multifunctional properties such as energy absorption, thermal isolation, anti-impact. The structural efficiency can be convincingly achieved by designing hierarchical cellular materials optimally even with moderate-quality constituents.

*Correspondence to: Weihong Zhang, Sino-French Laboratory of Concurrent Engineering, Northwestern Polytechnical University, 710072 Xi'an, China.
†E-mail: zhangwh@nwpu.edu.cn

Contract/grant sponsor: National Natural Science Foundation; contract/grant numbers: 10372083, 90405016
Contract/grant sponsor: Aeronautical Science Foundation; contract/grant number: 04B53080
Contract/grant sponsor: 973 Program; contract/grant number: 2006CB601205

Received 24 October 2005
Revised 28 February 2006
Accepted 7 March 2006

In recent years, topology optimization becomes an efficient approach to fulfil this task. Initially, it was developed to perform overall structural layout design where the macroscopic solid-void solution pattern is obtained by means of either the homogenization method [1–3], the solid isotropic material with penalization (SIMP) method with parametric material modelling [4, 5] or other methods like Voigt–Reuss mixing rule [6]. A survey of the previous work can be found in the work of Rozvany [7], Bendsøe and Sigmund [8].

Thereafter, successful applications are rapidly recognized for the purpose of tailoring effective properties of cellular materials. Among others, an inverse homogenization method was proposed by Sigmund [9], Sigmund and Torquato [10] and Silva *et al*. [11] as a material design procedure. The homogenization method that allows for establishing macroscopic effective properties of the heterogeneous medium in terms of microstructural variables is coupled with the SIMP method such that materials can be efficiently tailored to attain prescribed optimal microstructures or extreme properties. In contrast, the design of cellular structures, e.g. the cellular core of a lightweight sandwich panel for the compliance minimization corresponds to a multi-scale problem that is different from the pure material design and the pure structural topology optimization. Roughly speaking, it is an integrated design of both. The essential influence of underlying material microstructures upon global behaviours of macrostructures requires that microstructures must be designed to match optimally the loading and boundary conditions of the specific macrostructure. In this context, volume fractions of solid phases, the microstructure topology and the scale size of the material unit cell (MUC) have to be all taken into account simultaneously. Up till now, Fujii *et al.* [12] studied the compliance minimization problem of the macrostructure through topology optimization of material microstructures using the homogenization method. Rodrigues *et al.* [13] proposed a hierarchical computational procedure that integrates the global topology and local material optimal designs. As there may exist multiple solutions of microstructures that produce different local optimal effective elastic properties, Neves *et al.* [14] introduced the local buckling constraint to penalize the microstructure in the optimization procedure.

In fact, one important issue in the integrated design of materials and structures is concerned with the scale effect of MUC. This mechanism is confirmed from both micromechanics theories and experiments [15–18]. Nevertheless, few studies have been made so far about the scale effect of MUC upon topology design solution. In the elastic buckling design study by Bendsøe and Triantafyllidis [19], it was shown that the optimal size of MUC generally depends upon the overall dimension of the macrostructure and that the homogenization method is valid only when the MUC takes a size small enough.

As the homogenization method used in the above work is a two-scale asymptotic method based on the periodicity assumption of the MUC, the predicted effective properties only depend upon the material microstructure, volume fractions and properties of constituents. Such a method is correct only asymptotically so that results obtained preclude any scale effect in the real structure even for stiffness design. In other words, the homogenized descriptions are only valid when the size of the macrostructure is very large in comparison with the size of its material heterogeneities. In reality, this limit is never reached because the actual size of the MUC is not infinitely small and the macrostructure size is not infinitely large. Therefore in some problems, it is of great interest to formulate the integrated design problems with the retention of length-scale for a real structure. This is the motivation of the current work. Compared to the micromechanics methods of averaged field modelling summarized by Nemat-Nasser and Hori [20], the homogenization method is a general mathematics modelling method.

In this paper, an integrated optimization approach is proposed for the compliance minimization designs of 2D layered structures. The design procedure consists of two basic tasks: (1) the macroscopic design aiming at finding a preliminary layout of materials in the design domain globally; (2) the refined design determining locally the optimal material microstructure. The scale effect of the MUC or representative volume element (RVE) is captured by introducing the design element (DE) concept. This is why notions of MUC, RVE and DE are used interchangeably without strict distinction in the paper. Numerical results show that by changing the size as well as the aspect ratio of RVE, scale effects can be properly characterized in the final designs.

2. SCALE EFFECT OF THE MATERIAL MICROSTRUCTURE

A sandwich panel is illustrated in Figure 1. Assume that the hexagonal microstructure of the core material can take different scales but with the same volume fraction of the solid material. As a result, the whole structure may exhibit different mechanical performances under the specific loading. Recently, Tantikom *et al.* [17] also pointed out this phenomenon experimentally. As shown in Figure 2, the specimen with tubular core results in different nominal stress–strain curves when the number of cellular layers is changed but curves become indifferent whenever the number of cellular layers is large enough. This mechanism is the so-called scale effect as discussed by Burgueno *et al.* [18]. Therefore, when design optimization is concerned, the scale effect should be taken into account together with the morphology of the unit cell in a unified way.

However, as the homogenization method leads to the same effective elastic tensor in all above cases, its utilization is reasonable only when a considerable number of cells exist in the core. On the contrary, when the panel has only a few cellular layers, the scale effect becomes important in the design so that the predicted effective properties are unable to account for the actual state of the material.

To develop this study, consider the periodicity of the cellular microstructure in a given design domain shown in Figure 3. (Note $m = m_1 \times m_2$, with m_1 and m_2 being numbers of unit cells along direction x_1 and direction x_2, respectively.) For example, $m = 2 \times 4$ means that the design domain contains two unit cells in x_1 direction and four unit cells in x_2 direction, respectively. Without loss of generality, the scale-related design optimization may be interpreted as how to determine the number of unit cells m as well as the involved microstructure. In fact, such

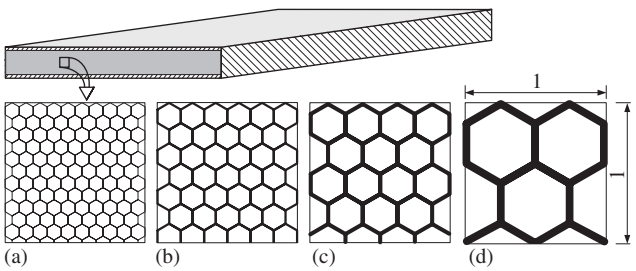

Figure 1. Scale effect of the cellular core with the same microstructure and volume fraction.

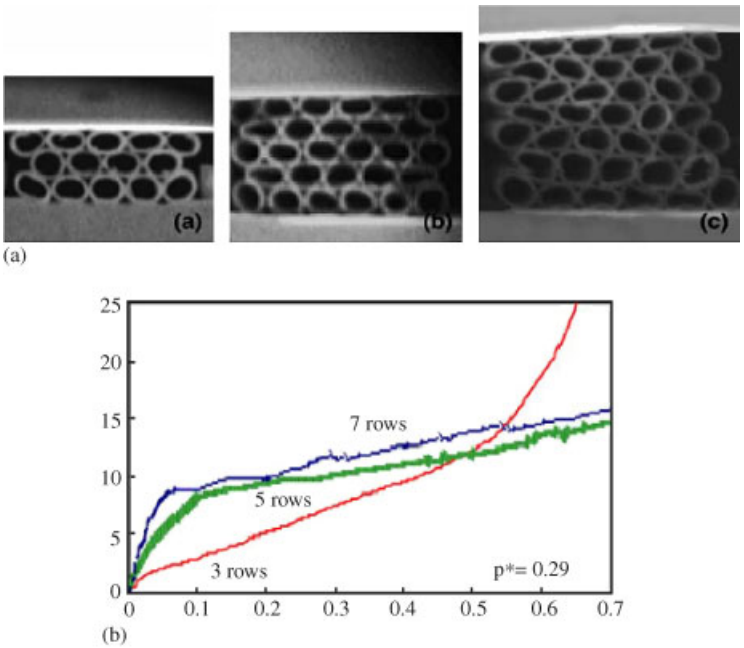

Figure 2. (a) Specimens with three, five and seven layers [17]; and (b) in-plane nominal compressive stress–strain curves of pure copper assemblies with different number of rows [17].

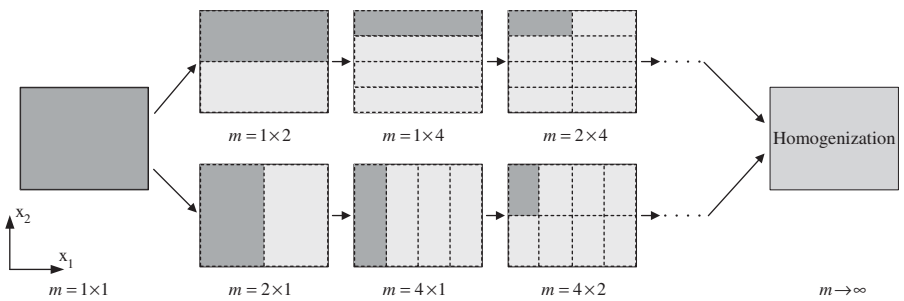

Figure 3. A two-dimensional domain with unit cells.

a scale-related problem reflects the intrinsic dependence between the material and structure. With the given material volume fraction, increasing m reflects reducing the small parameter ε defined as the ratio between the microscale of the material and the macroscale of the structure. In the limit case of $m \to \infty$, the scale effect will become ignorable and the design result converges to the asymptotic solution of the homogenization method. Alternatively, the limit case of $m = 1$ corresponds to the pure macroscale design. Meanwhile, for a fixed value of m, studies can also be carried out to analyse the influence of the aspect ratio of the unit cell upon the design of the microstructure.

3. THE HOMOGENIZATION METHOD WITH ASYMPTOTIC EXPANSION

As the proposed method will be compared with the homogenization method in this paper, a brief description of the latter is reminded here. The homogenization method is based on the two-scale asymptotic expansion of structural responses. Under the periodicity assumption of the MUC [1–3], each physical field, like the displacement of an arbitrary material point in a porous elastic body, can be approximated by an asymptotic expansion

$$u^{\varepsilon}(x) = u^0(x, y) + \varepsilon u^1(x, y) + \varepsilon^2 u^2(x, y) + \cdots \tag{1}$$

with x, the macroscopic variable measured in macroscale system (X), which varies slowly from unit cell to unit cell. $y = x/\varepsilon$, the periodic microscopic variable measured in microscale system (Y), which varies quickly within each unit cell. Parameter ε, the aspect ratio between the micro- and macroscale. Due to the complexity of analysing directly the cellular structure like that in Figure 1, overall performances of one such structure are often studied by modelling the cellular core as a homogenized medium with effective elastic tensor. This formulation is theoretically valid provided that $\varepsilon \ll 1$. As thoroughly explained in Reference [3], based on the asymptotic expansion of (1) and the elasticity equilibrium equation system defined over the unit cell

$$\int_Y E_{ijpq} \frac{\partial \chi_p^{kl}}{\partial y_q} \frac{\partial \upsilon_i}{\partial y_j} \, \mathrm{d}Y = \int_Y E_{ijkl} \frac{\partial \upsilon_i}{\partial y_j} \, \mathrm{d}Y \quad \forall \upsilon \in Y \tag{2}$$

the effective elastic tensor is as follows:

$$E_{ijkl}^H = \frac{1}{|Y|} \int_Y \left(E_{ijkl} - E_{ijpq} \frac{\partial \chi_p^{kl}}{\partial y_q} \right) \mathrm{d}Y = \langle E_{ijkl} \rangle - \langle \sigma_{ij}^{kl} \rangle \tag{3}$$

where $\langle E_{ijkl} \rangle$ denotes the averaged elastic tensor, which depends only upon the material volume fractions of constituents as evaluated by the classical mixture rule whereas $\langle \sigma_{ij}^{kl} \rangle$, the averaged stress tensor associated with the displacement vector χ^{kl} over the unit cell in load case kl, is a correction term reflecting the influence of the material microstructure of the unit cell. It is necessary to note that effective heat conductivity coefficients and thermal expansion coefficients of the MUC can be evaluated in a similar way.

4. SCALE-RELATED INTEGRATED DESIGN OF CELLULAR MATERIALS AND STRUCTURES

A cellular solid in the macroscale (X) with known boundary conditions and external forces is shown in Figure 4. According to the loading state of the structure, the optimal solution is to use a spatial distribution of heterogeneous cellular materials characterized by different microstructures at different locations of the design domain. Thus, materials will be optimally distributed to match the loaded regions. To do this, the design procedure is partitioned into two steps: macroscale layout design and refined optimization of the material microstructure.

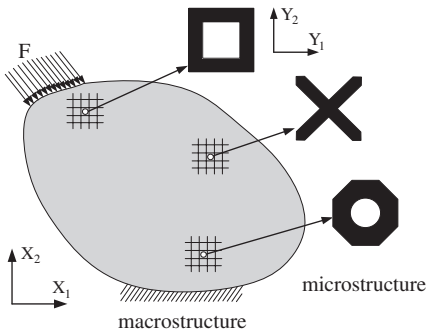

Figure 4. Illustration of a cellular domain with alternative material microstructures.

4.1. Macroscale layout design

Firstly, the macrostructure is considered as a homogenized body and is discretized into a finite element model. The overall behaviours can be determined by solving the corresponding FE equilibrium equation system

$$K(x)U(x) = F \tag{4}$$

For element i, suppose that the stiffness matrix, K_i, depends upon the element density variable x_i linearly, i.e. $K_i = x_i K_i^0$. This corresponds to the SIMP model in which the exponent $p = 1$ is used to ensure a smooth variation of the optimized density variables over the design domain. Note that K_i^0 is the stiffness matrix of the element with full solid material ($x_i = 1$). When the design task is to minimize the structural compliance subject to the volume constraint, the macroscale optimization model is expressed as

$$\begin{aligned} &\text{Min } C(x) = F^{\mathrm{T}} U(x) \\ &V(x) = \sum_{i=1}^{m} v_i^0 x_i \leqslant \overline{V} \\ &0 < \delta \leqslant x_i \leqslant 1, \quad i = 1, m \end{aligned} \tag{5}$$

where v_i^0 is the volume of element i with full material. $\overline{V}$ is the prescribed upper bound of the volume. $\delta = 10^{-4}$ is a small positive value used to prevent the singularity of the stiffness matrix. For 2D structures, the above formulation corresponds to exactly a traditional sizing optimization problem. As the number of design variables in (5) is far more than that of constraints, the problem will be solved in an efficient way by the dual approach [21, 22]. As shown below, it is mathematically demonstrated that the required sensitivity of the compliance objective function is always negative and can be easily obtained as a scaling of the strain energy of the concerned element.

$$\frac{\partial C}{\partial x_i} = F^{\mathrm{T}} \frac{\partial U}{\partial x_i} = F^{\mathrm{T}} K^{-1} \left(\frac{\partial F}{\partial x_i} - \frac{\partial K}{\partial x_i} U \right) = - U^{\mathrm{T}} \frac{\partial K}{\partial x_i} U = - \frac{1}{x_i} (F_i^{\mathrm{T}} U_i) = - \frac{1}{x_i} C_i \tag{6}$$

where it is supposed that the external force vector F is independent of the element density variables.

4.2. Refined topology optimization of material microstructures

Once the macroscale optimization problem (5) is solved, a global distribution of materials is obtained over the macrostructure. If values of design variables are $x_i = 0$ or 1, it means that element i is a void or solid element whereas $0<x_i<1$ means that the element has a cellular microstructure with intermediate densities, that needs to be identified further in the step of the refined microscale design. To this end, all parts of the macrocellular domain with $0<x_i<1$ $(i = 1, n)$ are firstly partitioned into DEs whose number and size can be determined following design specifications or available manufacturing capabilities. Meanwhile, each DE can be allowed to have its proper microstructure and each element i $(0<x_i<1)$ can be also regarded as an independent DE. Alternatively, one can also consider elements of the same values of x_i as a group of DEs having the common microstructure distributed periodically. To perform microstructure optimization, all DEs are considered to be an identical RVE that is further discretized into n finite elements with element density variables $y_{i,j}$ $(j = 1, n)$. Suppose that a number of m independent DEs exist, we can formulate the problem related to the overall structural compliance minimization in terms of $y_{i,j}$ $(i = 1, m;\ j = 1, n)$

$$
\begin{aligned}
&\min_{y} \Phi = -\sum_{i=1}^{m} U_i^{\mathrm{T}} K_i(y_i) U_i \\
&\sum_{j=1}^{n} v_{i,j}^0 y_{i,j} \leqslant v_i^0 x_i, \quad i = 1, m \\
&P(y_i) = \sum_{k=1}^{r} l_k (y_{i,j} - y_{i,j+1})^2 \leqslant \overline{P}, \quad i = 1, m \\
&0<\delta \leqslant y_{i,j} \leqslant 1, \quad j = 1, n, \ \ i = 1, m \\
&y_i = (y_{i,1}, \ldots, y_{i,j}, \ldots, y_{i,n})
\end{aligned}
\tag{7}
$$

where U_i corresponds to the known nodal displacement vector of DE i in the macroscale, that is obtained previously from (4) and (5). $y_{i,j}$ and $v_{i,j}^0$ are the microscale density design variable and element volume associated with finite element j involved in DE i, respectively. y_i is the vector composed of $y_{i,j}$ $(j = 1, n)$. $P(y_i)$ is a perimeter-like constraint devised to prevent the checkerboard phenomenon and intermediate densities in the final design pattern of the microstructure [23]. $\overline{P}$ is the given upper bound of the perimeter constraint. l_k is the element interface edge length between two adjacent elements. Clearly, the number of perimeter-like constraints equals the number of DEs having different microstructures. In comparison, the lack of such a perimeter-like constraint in (5) at the stage of macroscale layout design allows for the presence of intermediate densities whose microstructures will be figured out by solving (7). In addition, it proves easily that the perimeter-like constraint is a convex function as the Hessian matrix is semi-positive definite. For this reason, the dual approach [23] is selected as an efficient optimizer to solve (7).

Obviously, the objective function in (7) depends upon microscale density variables through stiffness matrices of DEs. Due to the separability of microscale variables of each DE, (7) can be equivalently decomposed into m independent subproblems and each of them corresponds to the minimization of the negative strain energy of the related DE. For the ith subproblem, we

have then

$$\begin{aligned}
&\underset{y_i}{\text{Min}}\ \Phi_i = -U_i^{\mathrm{T}} K_i(y_i) U_i \\
&\sum_{j=1}^{n} v_{i,j}^0 y_{i,j} \leqslant v_i^0 x_i \\
&P(y_i) = \sum_{k=1}^{r} l_k (y_{i,j} - y_{i,j+1})^2 \leqslant \overline{P} \\
&0 < \delta \leqslant y_{i,j} \leqslant 1, \quad j = 1, n \\
&y_i = (y_{i,1}, \ldots, y_{i,j}, \ldots, y_{i,n})
\end{aligned} \tag{8}$$

To figure out the optimal microstructure, material density variables y_i are penalized by the SIMP law ($p=4$) in the current design procedure. To perform sensitivity analysis of the objective function in (8), two approaches are set up as follows:

- *Scale-related approach*: For finite element j included in DE i, assume that the dependence of element stiffness matrix, $K_{i,j}$, upon its density variable, $y_{i,j}$, obeys the SIMP law with $K_{i,j} = y_{i,j}^p K_{i,j}^0$. Similarly to (6), the sensitivity of the objective function with respect to each microscale variable $y_{i,j}$ can be directly calculated as follows:

$$\frac{\partial \Phi_i(y_i)}{\partial y_{i,j}} = -U_i^{\mathrm{T}} \frac{\partial K_i}{\partial y_{i,j}} U_i = -U_{i,j}^{\mathrm{T}} \frac{\partial K_{i,j}}{\partial y_{i,j}} U_{i,j} = -\frac{p}{y_{i,j}} (U_{i,j}^{\mathrm{T}} K_{i,j} U_{i,j}) = -\frac{p}{y_{i,j}} C_{i,j} \tag{9}$$

  where $C_{i,j}$ and $U_{i,j}$ denote the strain energy and nodal displacement vector of finite element j included in DE i.
- *Homogenization approach*: When the DE is specified to have a size small enough, it can be thought to be a MUC for which the homogenization method can be applied to evaluate the effective elastic tensor E^{H}. Therefore, the stiffness matrix, K_i, of one such element depends upon microscale density variables, y_i, in such a way

$$K_i = \int B_i E^{\mathrm{H}}(y_i) B_i \, \mathrm{d}\Omega \tag{10}$$

  where B_i is the strain–displacement matrix. With the finite element discretization of DE i, the effective elastic tensor is evaluated from (3) in its discrete form

$$E^{\mathrm{H}} = \frac{1}{v_i^0} \sum_{j=1}^{n} \int [E_{i,j}(y_{i,j}) - E_{i,j}(y_{i,j}) B_{i,j} \chi_{i,j}(y_i)] \, \mathrm{d}\Theta \tag{11}$$

  with $E_{i,j}$ and $\chi_{i,j}$ being elastic constants and nodal displacement vector of finite element j involved in DE i.

In DE i, based on the SIMP law, $E_{i,j}(y_{i,j}) = y_{i,j}^p E_{i,j}^0$, used to describe the relation between the elastic tensor of finite element j and its density variable $y_{i,j}$, we can write the derivative of

E^{H} as

$$\frac{\partial E^{\mathrm{H}}}{\partial y_{i,j}} = \frac{1}{v_i^0}\left[\frac{p}{y_{i,j}} E_{i,j} v_{i,j}^0 - \frac{p}{y_{i,j}} \int E_{i,j} B_{i,j} \chi_{i,j}(y_i)\, \mathrm{d}\Theta - \sum_{j=1}^{n} \int E_{i,j} B_{i,j} \frac{\partial \chi_{i,j}}{\partial y_{i,j}}\, \mathrm{d}\Theta\right]$$

$$= \frac{1}{v_i^0}\left[\frac{p}{y_{i,j}} E_{i,j} v_{i,j}^0 - \frac{p}{y_{i,j}} \int \sigma_{i,j}(y_i)\, \mathrm{d}\Theta - \sum_{j=1}^{n} \int E_{i,j} B_{i,j} \frac{\partial \chi_{i,j}}{\partial y_{i,j}}\, \mathrm{d}\Theta\right] \tag{12}$$

where the partial derivative term, $\partial \chi_{i,j}/\partial y_{i,j}$, can be obtained by differentiating the equilibrium state equation of (2).

Now, based on these intermediate results, the chain rule will be finally applied for the differentiation of the objective function in (8) such that

$$\frac{\partial \Phi_i(y_i)}{\partial y_{i,j}} = -U_i^{\mathrm{T}} \frac{\partial K_i}{\partial y_{i,j}} U_i = -U_i^{\mathrm{T}} \left[\int B_i^{\mathrm{T}} \frac{\partial E^{\mathrm{H}}}{\partial y_{i,j}} B_i\, \mathrm{d}\Omega\right] U_i \tag{13}$$

Obviously, with the first approach, sensitivity analysis is simple to carry out.

4.3. Design optimization procedure

Based on the above developments, it is now possible to establish the overall optimization procedure that integrates both the macroscale layout design and refined microstructural design. The flowchart is shown in Figure 5.

As the design procedure is hierarchical and the computing task is time-consuming, periodic DEs are modelled as superelements to condense internal d.o.fs. In such a way, the FE analysis of the whole structure can be performed efficiently. Thereafter, at the local superelement level, a refined design of material microstructure will be carried out. To do this, the strain energy of each internal element included in the DE can be restituted and then introduced into (9) for sensitivity analysis.

5. NUMERICAL TESTS

Consider now a 2D rectangular domain of plane stress state shown in Figure 6. Assume that the design domain has a dimension of $L = 32$, $H = 20$ and a thickness of $t = 1$. The panel is loaded vertically with $F = 100$ (force/length). Young's modulus and Poisson's ratio of the material are $E = 1000$ and $v = 0.3$, respectively. Note that units are supposed to be consistent with SI system and omitted here. In this problem, a volume fraction of 60% is used for the solid phase in the design domain and the dimension of the DE, i.e. the RVE is noted by $l \times h$. For finite element modelling, if the vertical load is applied directly along the right edge where solid elements are eliminated during optimization, the problem will be ill-conditioned and become singular. To avoid this, a small non-designable elastic portion will be added artificially along one such edge to transfer the applied load.

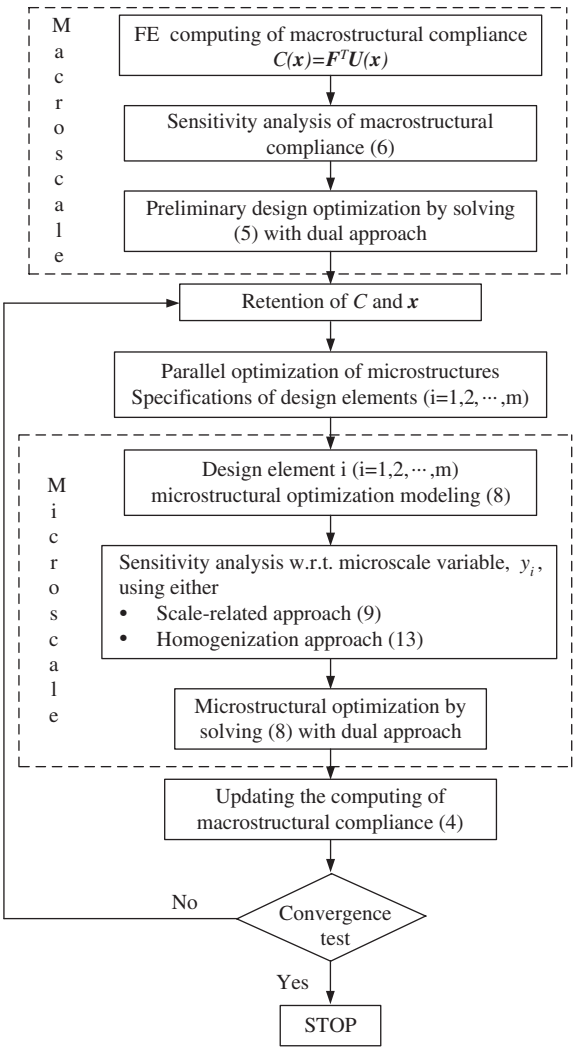

Figure 5. Integrated design of cellular materials and structures.

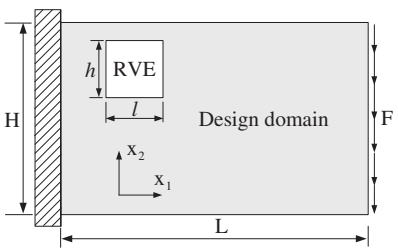

Figure 6. 2D rectangular domain.

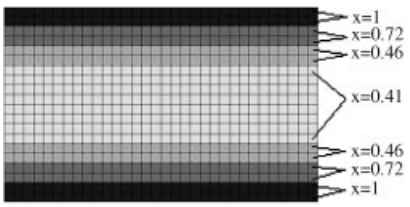

Figure 7. Macroscale design for material layout with SIMP model ($p = 1$).

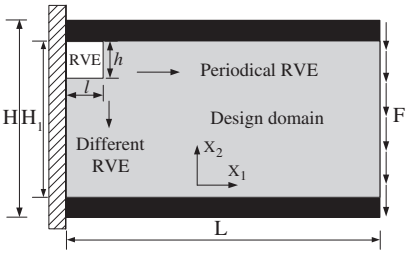

Figure 8. Design domain and RVE.

5.1. Macroscale layout design

The panel is macroscopically discretized into a mesh of 32×20 finite elements. Assume that elements in each horizontal layer take the same values of density variables that can be realized in way of design variable linking technique. In the 2D case, this is exactly equivalent to a thickness sizing problem. A number of 20 design variables of x_i $(i = 1, 20)$ exist totally. The optimal distribution of density variables is shown in Figure 7 after solving problem (5).

A symmetric distribution is obtained with x_i being $(1.0, 0.72, 0.46, 0.41, 0.46, 0.72, 1.0)$. Such a non-uniformly graded distribution is the stiffest one as expected to prevent the bending deformation from the engineering viewpoint.

5.2. Refined topology optimization of material microstructures for the cellular core

5.2.1. Case 1: scale effect of the MUC with graded material volume fractions. Following the result given in Figure 7, it is known that the refined design domain refers to the inner core of dimension $L \times H_1$ with values of density variables $(0 < x_i < 1)$ (Figure 8). Denote m and C_m to be the number of involved RVEs and the corresponding structural compliance, respectively. Suppose that the RVE is square and has a size of 2×2, then a number of $m = 16 \times 8$ RVEs exist, i.e. 16 RVEs along x_1 and eight RVEs along x_2, respectively. Moreover, RVEs in each horizontal layer are assumed to have a common microstructure (periodicity) along x_1 and to change along x_2. Consequently, eight independent subproblems of form (8) will be solved.

With the scale-related approach of Section 4.2, the optimal solution pattern that produces the minimum compliance of $C_{16 \times 8}$ is given in Figure 9(a). Comparatively, if the homogenization method of Section 4.2 is used and the effective elastic tensor is evaluated for each element of the mesh 32×20, the optimal solution denoted by C_∞ is shown in Figure 9(b).

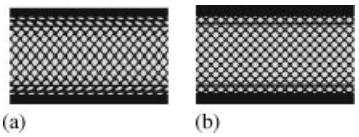

Figure 9. Comparison of scale-related design and homogenization approach: (a) $C_{16\times 8} = 172\,019.7$; and (b) $C_{\infty} = 172\,171.8$.

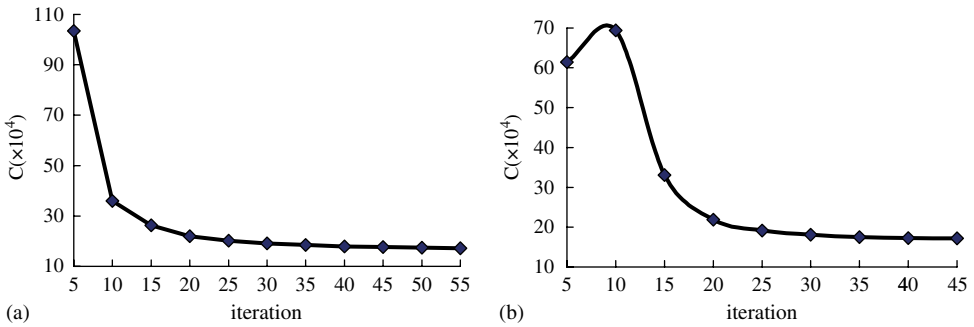

Figure 10. Iteration histories of: (a) scale-related design; and (b) homogenization approach.

One can see that microstructures change from one layer to another one in order that material capacities are fully explored to resist the bending force. Particularly, a lozenge microstructure is found along the neutral axis to resist the maximum shear stress. Note that although values of the structural compliance obtained by both approaches are very close, the difference still exists between microstructures. In both cases, iteration histories are finally shown in Figure 10. The convergence curves are found to be stable.

5.2.2. Case 2: scale effect of the MUC with constant material volume fraction. To reveal further the scale effect, another study is made now to show the influence of m upon the optimal designs of microstructures. Suppose that the inner core shown in Figure 8 has an averaged uniform value of density variables $\overline{x_i} = 0.5$ $(i = 3, 18)$ that corresponds to the same volume fraction (60%) over the whole structure but a volume fraction of 50% over the core. A common microstructure is assumed for all RVEs in the inner core. As a result, a variety of design solutions are obtained for square RVEs of different scales as shown in Figure 11. Related compliance values are plotted in Figure 12. The comparison shows that due to the successive size diminutions of the RVE, the design space is reduced and the number of constraints associated with the design variable linking augments so that the structural compliance (objective function) increases and converges to the solution of the homogenization method. This observation indicates that both material and structural designs can be unified from the viewpoint of the relative scale and that the solution of homogenization method is a limit case with $m = \infty$.

Moreover, it is interesting to analyse the effect of the aspect ratio l/h of the RVE upon the optimal design. By fixing the height value to be $h = 16$ and reducing the edge length of l gradually, different optimization results are given in Figure 13. Correspondingly, variations of the structural compliance versus m are plotted in Figure 14.

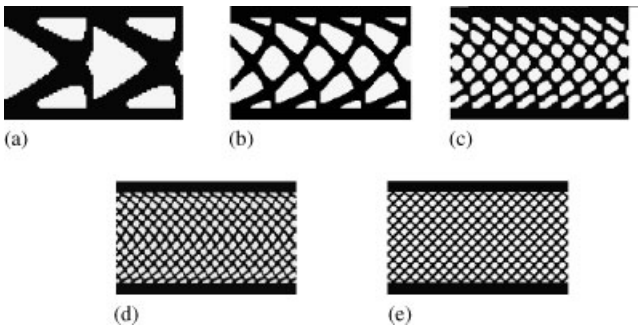

Figure 11. Scale effect of the square RVE on the core design result (core volume fraction 50%): (a) $C_{2\times1} = 165\,061.1$; (b) $C_{4\times2} = 168\,025.8$; (c) $C_{8\times4} = 176\,616.6$; (d) $C_{16\times8} = 181\,094.94$; and (e) $C_{\infty} = 186\,282.8$.

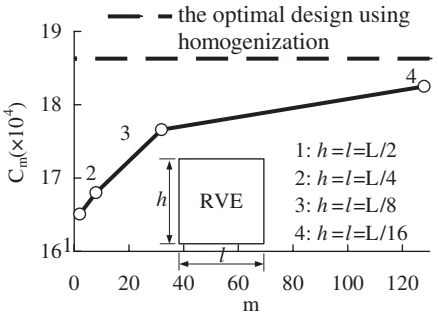

Figure 12. Compliance variation versus m.

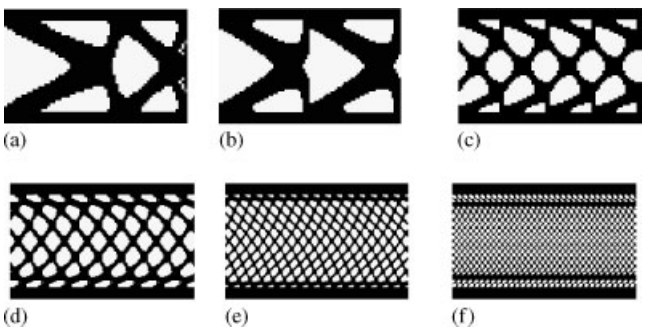

Figure 13. Effect of the RVE's aspect ratio on the core design result (core volume fraction 50%, $h = 16$): (a) $C_{1\times1} = 156\,015$; (b) $C_{2\times1} = 165\,061.1$; (c) $C_{4\times1} = 174\,745.9$; (d) $C_{8\times1} = 178\,483$; (e) $C_{16\times1} = 179\,108.9$; and (f) $C_{32\times1} = 181\,125.3$.

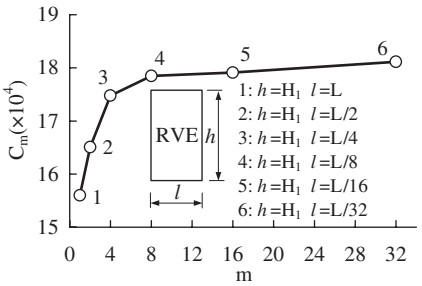

Figure 14. Compliance variation versus m.

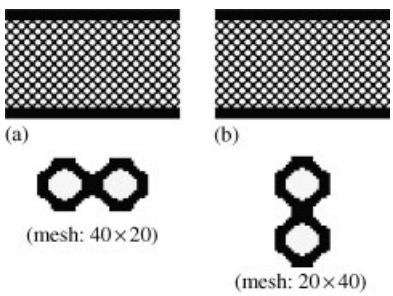

Figure 15. Topology optimization with the double of the basic square RVE: (a) $C_\infty = 186\,192$; and (b) $C_\infty = 186\,189$.

Furthermore, it is known that a square RVE of dimension $l \times h = 1 \times 1$ is usually used in the homogenization method to characterize the effective elastic tensor. Now, tests are made to rectangular RVEs that double the basic cell with dimensions $l \times h = 2 \times 1$ and 1×2, respectively for problem shown in Figure 8. In each case, a mesh of 40×20 and 20×40 finite elements are used. As shown in Figure 15, optimal results confirm that the homogenization method gives rise to the same topology design solutions.

5.3. Topology optimization of the whole panel with cellular materials

Now, the entire panel of dimension $L \times H$ will be fully designed with the cellular materials of identical microstructure instead of the inner core. Firstly, suppose that a square RVE will be used periodically along both x_1 and x_2 directions and the volume fraction is still kept to be 60%. In this case, the macroscopic design step related to (5) can be ignored. To study the scale effect, the size of the RVE will be reduced gradually. Corresponding optimal results are shown in Figures 16(a)–(c).

The influences of the aspect ratio, l/h, of the RVE is studied below in two cases. For $l = 16$, the stiffness of the structure reduces along with the increase of the aspect ratio l/h as illustrated in Figures 17 and 18. It is impossible to avoid appearance of useless horizontal stiffeners inside the domain due to the periodicity of the RVE along the vertical direction. For $h = 20$, the reduction of the aspect ratio l/h still leads to a diminution of the structural

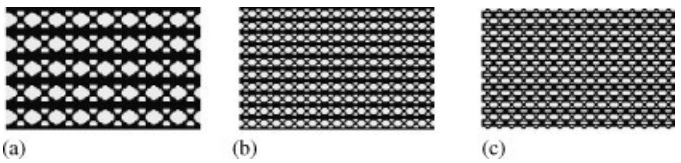

Figure 16. Scale effect of the square RVE on the design results: (a) $C_{8\times5} = 245\,925.4$; (b) $C_{16\times10} = 246\,045.2$; and (c) $C_{\infty} = 247\,230$.

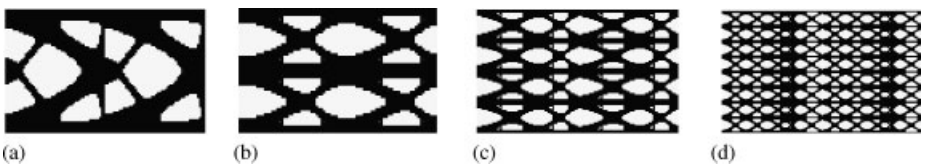

Figure 17. Effects of the aspect ratio of the RVE on the design results with $l = 16$: (a) $C_{2\times1} = 160\,797.3$; (b) $C_{2\times2} = 211\,017.9$; (c) $C_{2\times4} = 231\,804.3$; and (d) $C_{2\times8} = 2\,592\,998.7$.

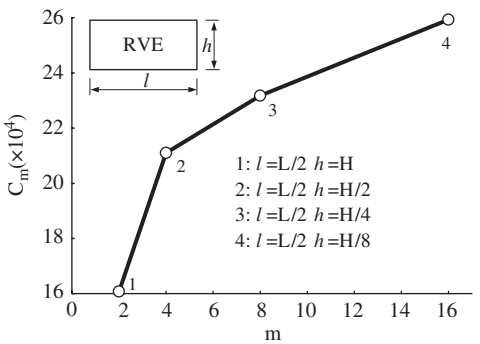

Figure 18. Compliance variation versus m with $l = 16$.

stiffness as shown in Figures 19 and 20. In both cases, with the refinement of RVE, the porosity distribution will become more and more important and solid stiffeners will become thinner.

5.4. Cellular structures with cyclic symmetry

The proposed DE approach can also be extended for the cellular core design of circular structures that find wide applications in the aerospace industry. The test is about a circular membrane with inner and outer skins as shown in Figure 21. It can also be regarded as a circular tube of infinite length (plane strain state). The inner hole and outer contour have the radii of $R_1 = 6$ and $R_2 = 12$, respectively. Two cases of different skin thickness ($t = 0.6, 1$) are investigated. Fixations will be imposed along the inner hole. Under the point-wise tangential loading of $F = 1600$ applied on the outer contour, the cellular core limited to a volume fraction of 40% needs to be designed for a maximum rigidity. To do this, the structure is partitioned into

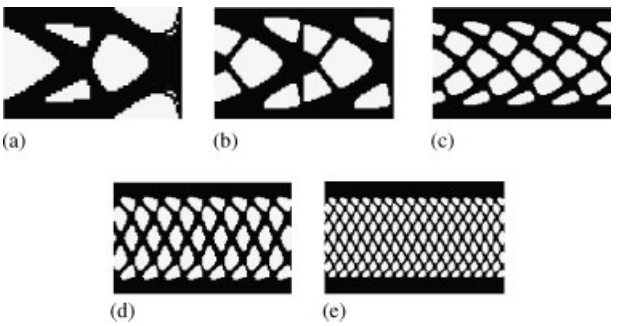

Figure 19. Effects of the aspect ratio of the RVE on the design results with $h = 20$: (a) $C_{1\times1} = 146\,774$; (b) $C_{2\times1} = 160\,797.3$; (c) $C_{4\times1} = 168\,666$; (d) $C_{8\times1} = 184\,585.2$; and (e) $C_{16\times1} = 185\,263.7$.

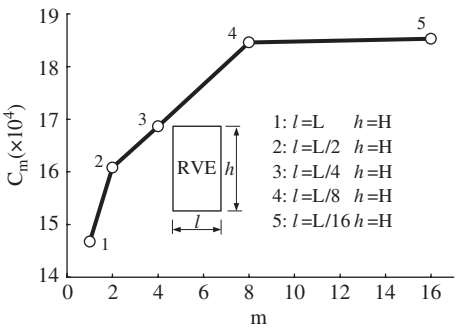

Figure 20. Compliance variation versus m with $h = 20$.

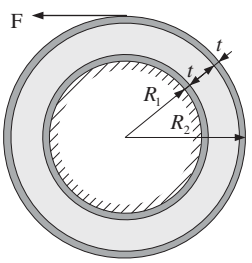

Figure 21. Cellular core design optimization.

16 representative sectors, i.e. DEs that hold the cyclic symmetry. By performing the refined design procedure using the scale-related approach, optimal design patterns are illustrated in Figure 22. It is found that stiffeners have a layout of being nearly perpendicular to each other like the classical solution of Michell truss structure [24]. Besides, both solutions are very similar except that small holes near the outer contour for solution with $t = 0.6$ are completely filled when $t = 1$. Alternatively, if a uniform pressure of $F = 100$ is applied along the inner

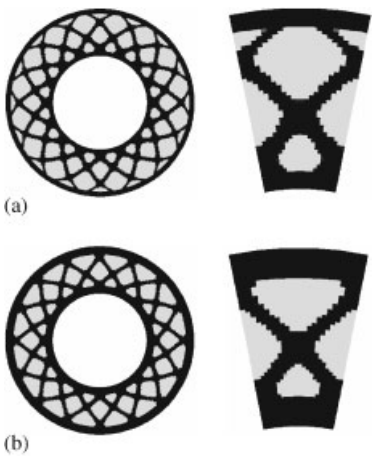

Figure 22. Optimal designs of cellular core: (a) $t = 0.6$; and (b) $t = 1$.

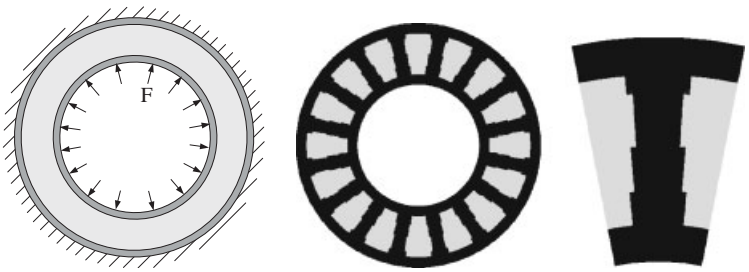

Figure 23. Optimal designs of cellular core for $t = 1$.

hole with fixations along outer boundary, optimal materials have a distribution uniquely along radial directions as shown in Figure 23.

6. CONCLUSIONS

The integrated design of materials and structures is studied in this paper. A two-level design methodology combining the macroscale material layout optimization with refined design of material microstructures is developed based on 2D examples. With the introduction of DE concept, we investigate the scale effect of the microstructure upon the optimal topology solution and we propose the superelement technique to improve the computing efficiency. Mathematical formulations of micro- and macroscale optimization problems are established together with sensitivity analysis. Based on 2D examples, it is shown that after the preliminary macroscale design, the initial attribution of layered RVEs is able to produce hierarchically graded material microstructures. Both the number and aspect ratio of the RVE have great influences upon the topology design results. In limit cases, the design becomes a pure topology optimization

problem of the macrostructure ($m = 1$) or a pure topology optimization problem of the material microstructure ($m = \infty$) equivalent to the homogenization solution. Therefore, it can be stated that designs of material microstructures and macrostructures are relative depending upon the scale. In addition, designs of periodical cellular structures can be easily extended to circular structures of cyclic symmetry. In all cases, clear black–white design patterns can be obtained and these solutions can be well adapted to the manufacturing capabilities.

ACKNOWLEDGEMENTS

The authors gratefully acknowledge the support of the National Natural Science Foundation of China (Grant Nos. 10372083, 90405016), the Aeronautical Science Foundation (Grant No. 04B53080) and 973 Program (Grant No. 2006CB601205).

REFERENCES

1. Bendsøe MP, Kikuchi N. Generating optimal topologies in structural design using a homogenization method. *Computer Methods in Applied Mechanics and Engineering* 1988; **71**(2):197–224.
2. Bensoussan A, Lions JL, Papanicolaou G. *Asymptotic Analysis for Periodic Structures*. North-Holland: Amsterdam, 1978.
3. Sanchez-Palencia E. *Non-homogeneous Media and Vibration Theory*. Lecture Notes in Physics, vol. 127. Springer: Berlin, 1980.
4. Bendsøe MP. Optimal shape design as a material distribution problem. *Structural Optimization* 1989; **1**: 193–202.
5. Rozvany GIN, Zhou M, Birker T. Generalized shape optimization without homogenization. *Structural Optimization* 1992; **4**:250–254.
6. Swan CC, Kosaka I. Voigt-Reuss topology optimization for structures with linear elastic material behaviours. *International Journal for Numerical Methods in Engineering* 1997; **40**:3033–3057.
7. Rozvany GIN. Aims, scope, methods, history and unified terminology of computer-aided topology optimization in structural mechanics. *Structural and Multidisciplinary Optimization* 2001; **21**:90–108.
8. Bendsøe MP, Sigmund O. *Topology Optimization*: *Theory*, *Methods and Applications*. Springer: Berlin, 2003.
9. Sigmund O. Materials with prescribed constitutive parameters: an inverse homogenization problem. *International Journal of Solids and Structures* 1994; **31**(17):2313–2329.
10. Sigmund O, Torquato S. Design of materials with extreme thermal expansion using a three-phase topology optimization method. *Journal of the Mechanics and Physics of Solids* 1997; **45**(6):1037–1067.
11. Silva ECN, Fonseca JSO, Kikuchi N. Optimal design of piezoelectric microstructures. *Computational Mechanics* 1997; **19**(5):397–410.
12. Fujii D, Chen BC, Kikuchi N. Composite material design of two-dimensional structures using the homogenization design method. *International Journal for Numerical Methods in Engineering* 2001; **50**: 2031–2051.
13. Rodrigues H, Guedes JM, Bendsøe MP. Hierarchical optimisation of material and structure. *Structural and Multidisciplinary Optimization* 2002; **24**:1–10.
14. Neves MM, Sigmund O, Bendsøe MP. Topology optimization of periodic microstructures with a penalization of highly localized buckling modes. *International Journal for Numerical Methods in Engineering* 2002; **54**:809–834.
15. Sutherland LS, Shenoi RA, Lewis SM. Size and scale effects in composites—I. Literature review. *Composites Science and Technology* 1999; **59**:209–220.
16. Pecullan S, Gibiansky LV, Torquato S. Scale effects on the elastic behavior of periodic and hierarchical two-dimensional composites. *Journal of the Mechanics and Physics of Solids* 1999; **47**:1509–1542.
17. Tantikom K, Aizawa T, Mukai T. Symmetric and asymmetric deformation transition in the regularly cell-structured materials. Part I: experimental study. *International Journal of Solids and Structures* 2005; **42**: 2199–2210.
18. Burgueno R, Quagliata MJ, Mohanty AK, Mehta G, Drzal LT, Misra M. Hierarchical cellular designs for load-bearing biocomposite beams and plates. *Materials Science and Engineering A* 2005; **390**(1–2):178–187.

19. Bendsøe MP, Triantafyllidis N. Scale effects in the optimal design of a microstructured medium against buckling. *International Journal of Solids and Structures* 1990; **26**(7):725–741.
20. Nemat-Nasser S, Hori M. *Micromechanics*: *Overall Properties of Heterogeneous Materials*. Elsevier: Amsterdam, 1993.
21. Fleury C, Braibant V. Structural optimization: a new dual method using mixed variables. *International Journal for Numerical Methods in Engineering* 1986; **23**:409–428.
22. Beckers M. Dual methods for discrete structural optimization problems. *International Journal for Numerical Methods in Engineering* 2000; **48**:1761–1784.
23. Zhang WH, Duysinx P. Dual approach using a variant perimeter constraint and efficient sub-iteration scheme for topology optimization. *Computers and Structures* 2003; **81**(22/23):2173–2181.
24. Michell AGM. The limit of economy of material in frame structures. *Philosophical Magazine* 1904; **8**(6): 589–597.

